Department of Electrical
and
Computer Systems Engineering

Technical Report
MECSE-16-2003

Grating-Assisted Fibre-Slab Couplers

Le Nguyen Binh and Shu Zheng

MONASH
UNIVERSITY

Grating-Assisted Optical Fibre-Planar Waveguide Coupling Systems

L. N. Binh and S. Zheng

Department of Electrical and Computer Systems Engineering, Monash University, P.O. Box 35, Clayton, Victoria 3800, Australia. e-mail: le.binh@eng.monash.edu.au

Abstract

Coupled-mode equations for an asymmetric fibre-to-planar optical coupling system, incorporated a grating structure are presented. A grating-assisted coupling coefficient is described. When the parameters of the coupler are such that there is no phase synchronism between the fibre and the slab modes, the grating enhances the coupling in both the resultant amplitude and phase modulation. However, when there is a phase synchronism between the two sets of guided modes of the circular fibre and planar slab structures, the effects of the grating structure are greatly reduced. The coupling features give the fibre-slab coupler another unique dimension of amplitude and phase modulation and thus increase the coupler design flexibility to achieve certain desired level of power transfer from one waveguide structure to the other and vice versa.

Keywords: *Optical fibres, planar optical waveguides, integrated optics, optical couplers*

1 Introduction

Current dynamic development of the high capacity reaching an order of a few tera-bps optical networks leads to intensive search for optical components that can simultaneously demultiplex optical wavelength channels and spatially distribute them into appropriate output channel waveguide structures. Grating couplers are expected to provide optical components for such wavelength multiplexing and demultiplexing demands, in particular a number of

optical components for wavelength add-drop multiplexers. Recently interests have also been focused in the search of efficient optical couplers for fulling the demand of add/drop filters and receivers[1,2] for wavelength division multiplexing optical communications.

Directional couplers made of non-identical and asymmetric optical waveguides, including cases of grating assistance and non-assistance, have been investigated[3,4] analytically. In such coupling systems the coupled equations between guided modes which are not orthogonal due to the non-identical properties of optical waveguides, a planar waveguide and a circular optical waveguiding structure, lead to a number of interesting effects such synchronised coupling and branching.

Optical physical grating can assist the coupling systems between optical waveguides in selection of a particular wavelength and divergence of its power in one branch to the other of the coupled system. There are several possibilities of optical coupling systems such as fibre-to-fibre and slab-to-slab in integrated photonics and a composite fibre-to-slab waveguide coupling systems. The latter system is considered in this paper, that is an optical coupling system with the slab waveguide incorporating with a grating structure. This structure would find important applications in optical wavelength demultiplexing system by performing the function of filtering and spatial splitting to different directions in the slab waveguide and then coupled to optical channel waveguide sections, that is similar mechanism as in the array waveguide gratings.

In this paper we present a coupled-mode analysis for such grating-assisted fibre-slab couplers. First, the analytical expressions of the scalar coupled-mode equations (CME) and the system coupling coefficients are given, based on a scalar and simplified coupled-mode formulations[5]. Secondly, the analytical expressions of the coupling coefficients due to the presence of the grating are obtained and numerical algorithm for the solutions of the new coupled-mode equations are described. Finally, the numerical calculations and discussion are

carried out to reveal the grating-assisted coupling features. We note also that only the evolution of the optical powers in the waveguide systems is considered in this paper. The filtering and demultiplexing of different channels are considered in another article.

2 Coupled Mode Equations and Coupling Coefficients

A grating-assisted fibre-slab waveguide is a general asymmetric and composite coupling system. For simplicity, a scalar coupled-mode approach is formulated, with additional coupling coefficients analytically derived. This is followed by numerical examples to demonstrate the effects of the grating structure on the mode (power) coupling between the guided fibre and slab modes.

A scalar formulation of CME is adopted in analysing the grating assisted coupling systems with the fundamental equations derived in Ref.[5] for the coupling system between an optical fibre and a planar slab optical waveguide. The correctness of the scalar approximation, owing to the range of the structural and optical constants of the fibre-slab coupler system has been studied in details. Scalar coupled-mode equations with grating-assisted couplings can be derived straightforwardly with additional coupling coefficients that are described here in this section. If the fibre and the planar waveguide are brought close to each other the evanescent fields of the two waveguiding systems are overlapped and the two waveguides are perturbed or coupled. The coupling in this case is occurring between two set of non-orthogonal guided modes in addition of a geometrically perturbed structures of the grating.

The effect of the grating perturbation can be expressed as an axial perturbation on the index profile of the fibre-slab coupler

$$n_g^2(x,y,z) = n^2(x,y) + \Delta n^2(x,y,z) \qquad (1)$$

with a weak perturbation of

$$\Delta n(x,y,z) << n(x,y) \qquad (2)$$

and with n_g represents the index profile of the whole fibre-slab coupler with grating, whilst n represents that of the whole coupler without grating. Assuming a grating of rectangular shape, Figure 1(a) illustrates the cross sectional view along the propagation direction z of such coupler with the boundary (solid line) of the grating and that (dashed line) of the unperturbed coupler without the grating, while Figure 1(b) shows the cross sectional view of the transverse plane of the fibre-planar coupling system without the additional grating structure. Note that the different sections of the periodic grating structure are marked by the sign + and - at which both the index perturbation $\Delta n^2(x,y)$ and the fields are different[4]. In addition, Λ_+ and Λ_- are the corresponding periods of the grating, and *2d* indicates the depth of the grating and K_g ($= 2\pi/\lambda$) the grating equivalent wave number. Such grating assisted fibre-planar waveguide coupling system can be fabricated by using a polished cladding circular core fibre overlaid by an light-induced grating written in an organic polymer thin film and covered with another thin film layer acting as a planar waveguide.

In order to obtain simplified scalar formulations of coupled mode and compound mode theories, instead of the rather cumbersome vectorial approaches, the common well known scalar approximations of weakly guiding of the fibre and planar waveguides for a weakly coupling are assumed[7,8]. Assuming that there is only the dominant linearly polarised fundamental mode of the fibre LP_{01} which could be initially excited in the fibre, the transverse electric field in the grating assisted/perturbed and coupled fibre-planar waveguide coupling system can be represented by the superposition of the guided modes of the fibre, the planar slab waveguide. The assistance of the coupling via the grating can be considered as an additional perturbation to be included in the wave equation.

The scalar coupled-mode equations for a fibre-planar waveguide coupling system can be obtained by modifying the coupled mode equations of a fibre-slab coupling system as given in

Appendix 1 equations (A7.a) and (A7.b), with additional coupling coefficients due the presence of the grating perturbation as

$$a_{0\pm}' = -j[\beta_{f00}+Q_{f00}+Q^{(g)}_{f00\pm}]a_0 - j\sum_n [K_{f0n}+K^{(g)}_{f0n\pm}]b_n \quad (3a)$$

$$b_{m\pm}' = -j\sum_n [\delta_{mn}\beta_{sn}+Q_{smn}+Q^{(g)}_{smn\pm}]b_{n\pm} - j[K_{sm0}+K^{(g)}_{sm0\pm}]a_{0\pm} \quad (3b)$$

where $j=\sqrt{-1}$, the ± sign indicates the alternating regions of the gratings with respect to the non-grating level (dashed referenced line). $a'_{0\pm} = \frac{da_{0\pm}}{dz}$ i.e. the evolution of the amplitude of the field propagating in the optical fibre and $b'_{m\pm} = \frac{db_{0\pm}}{dz}$ or the evolution of the amplitude of the optical field of mth order mode along the propagation direction. *m,n = 0,1,2, …* indicate the mode order number of the guided mode spectrum of the planar slab waveguide, δ_{mn} is the Kronecker delta function indicating the possibility of the cross coupling between modes of the slab waveguide. $\{Q_{f00\pm},Q_{smn\pm}\}$ and $\{K_{f0n\pm},K_{sm0\pm}\}$ are the self- and cross-coupling coefficients of the coupler when the grating is removed and their analytical expressions are given in the Appendix. The superscript g indicates the contribution to the coupled equations due the presence of the grating and the subscripts *f* and *s* indicate the contribution due to the fibre and slab waveguides respectively. Thus $\{Q^{(g)}_{f00\pm},Q^{(g)}_{smn\pm}\}$ and $\{K^{(g)}_{f0n\pm},K^{(g)}_{sm0\pm}\}$ are the additional self- and cross-coupling coefficients due to the presence of the *grating perturbation* and defined by, respectively

$$Q^{(g)}_{f00\pm} = \frac{k^2}{2\beta_{f0}}\int_{A_\infty} \Delta n^2(x,y,z)\, F_{0\pm}{}^2 \mathrm{d}A \quad (4a)$$

$$Q^{(g)}_{smn\pm} = \frac{k^2}{2\beta_{sm}}\int_{A_\infty} \Delta n^2(x,y,z)\, S_{m\pm}S_{n\pm} \mathrm{d}A \quad (4b)$$

$$K^{(g)}_{f0n\pm} = \frac{k^2}{2\beta_{f0}} \int_{A_\infty} \Delta n^2(x,y,z)\, F_{0\pm} S_{n\pm} \mathrm{d}A \tag{5a}$$

$$K^{(g)}_{sm0\pm} = \frac{k^2}{2\beta_{sm}} \int_{A_\infty} \Delta n^2(x,y,z)\, S_{m\pm} F_{0\pm} \mathrm{d}A \tag{5b}$$

Analytical solutions of the above-defined additional coupling coefficients are dependent on the expression of $\Delta n^2(x,y,z)$, i.e. the cross-sectional locations as well as the longitudinal profiles of the grating perturbation. The index modulation by the grating structure, such as that produced by induced UV written techniques, can be approximately expressed as[9]

$$\Delta n^2(x,y,z) \propto \cos(K_g z) \tag{6}$$

and using (4) and (5), the grating-induced coupling coefficients can be obtained as

$$Q^{(g)}_{f00\pm} = \frac{k^2}{2\beta_{f0}} (n_c^2 - n_s^2)\cos(K_g z) \int_{a+s-d}^{a+s+d} \mathrm{d}x \int_{-\infty}^{\infty} \mathrm{d}y\, F_0^2(x,y) \tag{7a}$$

$$Q^{(g)}_{smn\pm} = \frac{k^2}{2\beta_{sm}} (n_c^2 - n_s^2)\cos(K_g z) \int_{a+s-d}^{a+s+d} \mathrm{d}x \int_{-\infty}^{\infty} \mathrm{d}y\, S_{m\pm} S_{n\pm} \tag{7b}$$

$$K^{(g)}_{f0n\pm} = \frac{k^2}{2\beta_{f0}} (n_c^2 - n_s^2)\cos(K_g z) \int_{a+s-d}^{a+s+d} \mathrm{d}x \int_{-\infty}^{\infty} \mathrm{d}y\, F_0 S_{n\pm} \tag{8a}$$

$$K^{(g)}_{sm0\pm} = \frac{k^2}{2\beta_{sm}} (n_c^2 - n_s^2)\cos(K_g z) \int_{a+s-d}^{a+s+d} \mathrm{d}x \int_{-\infty}^{\infty} \mathrm{d}y\, S_{m\pm} F_0 \tag{8b}$$

These integrals can be analytically solved and closed-form expressions of the additional coupling coefficients can be obtained. The effects of grating on the mode power coupling can now be investigated via numerical calculations of the scalar coupled-mode equations described in (3). Note, however, that the coupled-mode equations with the sub-index + and -

have to be used periodically in the grating sections Λ_+ and Λ_-, respectively, along the propagation direction.

3 Numerical Results and Discussions

Numerical calculations are carried out in comparison with our results of the simplified scalar CME for fibre-slab couplers without grating structure as briefly described in Appendix 1.

3.1 Effects on Mode Coupling

All the numerical calculations have been conducted under practical conditions at an optical wavelength λ = 1.55 μm. The composite asymmetric coupler consists a fibre radius a = 2.5 μm, a slab waveguide of thickness t = 3 μm. The refractive index of the fibre cladding n_c is 1.46 and the refractive index of the slab guide n_s = 1.4745. The separation distance, s, between the fibre and the slab is *500 nm*. Numerical examples are first calculated when the refractive index of the fibre core n_f is varied against that of the slab guide n_s so that the modulation of the grating with different coupling conditions can be directly observed. The initial values for the grating are (1) the grating-depth $2d = 1.0\ \mu m$ (2) the grating wave-number $K_g = |\beta_{f0}-\beta_{s0}|$. Figure 2 demonstrates the interesting effects of grating on the coupling when the index of refraction $n_f = 1.4817$, 1.4756 and 1.4709, respectively, whilst the slab-guide refractive index is kept constant $n_s = 1.4745$. This can be equivalent to the variation of refractive index of the planar waveguides as a function of the optical spectrum of lightwaves. The perturbation of the grating on the asymmetric fibre-slab guided-wave coupler obviously changes both the power-beating lengths and the coupling strength. Figure 2(a) shows that, when $n_f > n_s$, the grating has approximately doubled the power-beating length whilst strengthening the coupling between the fibre and slab modes. Note that the periodic index modulation of the fibre-slab coupler structure also affects the power coupling resulting in intermittent zig-zag shaped modulations on the mode-power $|a_0|^2$. Additional ripples of the

optical power travelling in the fibre have also been observed and this phenomenon is due to additional scattering the lightwaves into other guided modes of the planar wavguides. These ripples become more evident as the difference in the refractive indices of the fibre and the planar waveguides is getting smaller.

The effect of the grating-assisted coupling is more evident when $n_f = 1.4756$, as shown in Figure 2(b). According to the scalar CME, the coupler *without* grating is not phase matched (although close) between the fibre and the slab modes and, as a result, more than 50% of the launched power remains in the fibre. However, for the coupler *with* a grating, the phase matching is introduced via the value of K_g of the grating and the coupling is therefore assisted leading to a complete power transfer from the fibre to the slab after certain distance of propagation of around *6mm*. Evidence of higher degrees of ripples of the optical power propagating along the fibre guide indicates strengthening of coupling between the fibre mode and other modes of the planar guide.

Finally, when $n_f < n_s$, there is a phase match between the fibre mode and one of the transverse slab modes even at the absence of the grating structure. It can be seen that the additional phase match between the fibre mode and the lowest-order slab transverse slab mode does not 'assist' the coupling much at all. Instead, it appears that the grating manifests its effect mainly through the phase modulation, i.e. altering the values of beat length, whilst slightly tuning the power decay in the fibre and the level of power transfer from the fibre to the slab. However the power ripples are getting stronger than the other two cases, thus the coupling of the fibre mode to other modes of the planar guided mode spectrum are also happening and exist for all grating assisted fibre-slab coupler. These random cross couplings may enhance the unwanted cross coupling between the guides and their impact on the multi-wavelength optical system switching/broadcasting would be further investigated in a future article.

3.1 Effects of Grating Parameters

Two grating parameters, expected to be most influential on the coupling of the fibre-planar waveguide coupling systems are the grating period and the grating depth. Their effects on the power coupling between guided modes of the waveguides of the coupler are considered separately.

3.1.1 Effects of Grating Period

Firstly, comparison is made when the depth of the grating is fixed whilst the period of the grating is set as $pd_1 = 2\pi/|\beta_{f0}-\beta_{s0}|$ and $pd_2 = 2\pi/|\beta_{f0}-\beta_{s10}|$, respectively. That is, the wave number of the grating, K_g, is set to compensate the phase mismatch between the propagation constant of the fundamental linearly polarised mode of the fibre and transverse slab guided mode (i.e. $|\beta_{f0}-\beta_{s0}|$), and that between the fibre guided mode and the 11^{th} slab transverse guided mode (*i.e.* $|\beta_{f0}-\beta_{s10}|$). The effect of a small variation of the grating period can be illustrated. It can be seen from Figure 3 that, when $n_f > n_s$, curves of group (1) shows that the grating-assisted couplings have similar patterns of the power modulation, with about 10% less power coupled from the fibre to the slab when the grating-period ($2\pi/K_g$) is decreased from pd_1 to pd_2. When $n_f < n_s$, there is already a phase-match between the fundamental fibre guided mode and one of the transverse slab modes and the curve-group (2) reveals that the grating-introduced phase-compensation does not alter the coupling properties as much as it does in the case of the curve group (1). No significant effects of the grating period on the power coupling can be observed in this case. That is, the diagrams of fibre mode-power $|a_o(z)|^2$ appear indistinguishable from those of couplers without gratings (with n_o= *1.46* and *1.47*).

Secondly, comparison is made when the depth of the grating is fixed whilst the period of the grating is set to $2\pi/|\beta_{f0}-\beta_{s0}|$ and *160* (μm) (much smaller than $2\pi/|\beta_{f0}-\beta_{s0}|$). This is to show the effect of a large variation of the grating period. The modulation on power coupling due to the

large variation of the grating period is clearly observed in Figure 4. The dashed curves indicate the reduction of both the grating period in modulations of the power coupling and the amount of power being transferred from the fibre to the slab. Similar to Figure 3, the grating effect appears stronger when there is no exact phase match for the coupler at the absence of the grating structure.

Both Figures 5 (a) and (b) show that, in these cases, the effects of the grating-period variation are very small in comparison to the case when $n_o = 1.40$. This may be explained by the fact that, at the absence of the grating structure, the coupler system is already in, or close to, a phase matching between the fibre mode and the transverse slab guided modes. As a result, the natural coupling (i.e. coupling without the aid of the grating) becomes dominant and the mechanism of grating-assisted coupling is suppressed.

3.1.2 Effects of Grating Depth

Comparison is made when the period of the grating is fixed, whilst the depth is varied from

$d = 0.05\ \mu m$ to $d = 0.025\ \mu m$. Figure 6 displays changes of power modulations either when $n_f > n_s$ (i.e. no fibre-slab phase synchronism) or $n_f < n_s$ (i.e. possible fibre-slab phase synchronism). Similar to Figure 3, it demonstrates that the effect of the grating is reduced when there is a phase match between the fibre and slab modes at the absence of the grating (see Figure 6, curves indicated with (2)).

4 Concluding remarks

Grating-assisted coupling in a composite asymmetric optical waveguiding system is analysed utilising the improved scalar CME whilst treating the effect of grating as a periodic perturbation on the index profile of the whole coupler structure. The coupled-mode equations for the fibre-slab coupler with grating can be described in a similar way as those without

grating, but with the coupler index profile overlaid by a periodic index modulation in each of the analytical expression of coupling coefficients as usually found in couplers without gratings. Additional grating-assisted coupling coefficients are obtained as additional features to that of the case of non-grating assisted. When the parameters of the coupler are such that there is no phase synchronism between the fibre and the slab modes, the grating enhances the coupling as seen in both the resultant amplitude and phase modulation. However, when there is a phase synchronism between the two sets of guided modes of the asymmetric optical waveguides, the effects of the grating structure are greatly reduced, i.e. the grating in this case does not strongly assist the coupling, if at all. This leads to a possibility of tuning the gratings for switching such as thermal tuning of the refractive index of the slab structure. Faster switching device can be generated if such tuning can be conducted via an excitation of an optical pulse guiding though the slab, e.g. an organic thin film, that exhibits a nonlinear third order effect.

Evidence of the coupling of the fibre mode to other guided modes of the mode spectrum of the planar waveguides has been observed in all structures of the grating-assisted couplers but varied according to the effectiveness of the phase matching between the fibre mode and the components of the multimode spectrum due the difference on the refractive indices between the fibre and the planar waveguides.

The above coupling features add to the fibre-slab coupler another unique dimension of amplitude and phase modulation and thus increase the flexibility of system design to achieve the desired level of power transfer from the fibre to the slab waveguide. This may find practical applications in design or analysis of general asymmetric or hybrid waveguide couplers.

5 References

[1] Jan, Y.H., Heimuch, M.F., Coldren L. and DenBaars, S.P. "Wavelength-selective grating assisted co-directional coupler tunable receiver on InP/InGaAsP", Elect. Lett., vol.32, no. 6, 199 , pp. 593-594.

[2] Bakhti, F., Snansonetti, P., Sinet C., Gasca, L., Martineau, L., Lacroix, S., Daxhelet , X. and Gonthier, F. , "Optical add/drop multiplexer based on UV-written Bragg grating in a fused 100% coupler", Elect. Lett., vol. 33, 1997, pp. 9-10.

[3] Marcuse, D., "Directional couplers made of non-identical asymmetric slabs: Part I: synchronous couplers", IEEE J. Lightw. Tech., vol. LT-5, no. 1, pp. 113-118, 1987.

[4] D. Marcuse, D., "Directional couplers made of non-identical asymmetric slabs: Part II: grating assisted couplers", IEEE J. Lightw. Tech., vol. LT-5, no. 1, pp. 113-118, 1987.

[5] Zheng, S., Binh, L.N. and G.P. Simon, "Composite optical fibre-slab waveguides – Ascalar coupled mode analysis with vector correction", Opt. Quant. Electron., vol. 29, 1997, pp. 671-682.

[6] Hong, J. and Huang, W. P., "Asymmetric power coupling in grating-assisted couplers" *IEE Proc. Optoelectron*., vol. 142, No.2, 1995, pp.103-108.

[7] D. Glodge "Weakly guiding fibers", Appl. Opt., vol. 10, pp. 2252-2258, 1971.

[8] A.W. Snyder and J.D. Love, "Optical Waveguiding Theory", Chapman and Hall, London, 1983.

[9] Grieffel, G., Itzkovitch, M. and Hardy, A., "Coupled-mode formulation for directional couplers with longitudinal perturbations", IEEE *J. Lightw. Tech.,* Vol. 27, 1991, pp. 985-994.

[10] Snyder, A.W. and Ankiewicz, A., "Optical Fibre Couplers – Optimum Solution for Unequal Cores", IEEE J. Lightw. Tech., vol. 6, pp. 463-474, 1988.

[11] Marcuse, D., "Investigation of coupling between a fibre and an infinite slab", IEEE J. Lightw. Tech., vol. LT-5, pp. 268-273, 1989.

[12] Marcuse, D., Personal Communications in relation to errors in paper of Marcuse [11].

6 Appendix 1: Coupled Mode Equations for Non-grating Fibre-Slab Coupling System

The transverse electric field in the coupled fibre and slab waveguides can be well represented by the superposition of the guided-modes of the fibre and the slab, i.e. $\{F_0, S_n\}$

$$E(x,y,z) = a_0(z)F_0(x,y) + \sum_n b_n(z)S_n(x,y) \tag{A1}$$

where $\{a_0(z), b_n(z)\}$ $(n = 0, 1, 2, \cdots)$ is a set of z-dependent expansion (excitation) coefficients (modal amplitudes), whilst the summation is carried out over the set of discretised transverse slab modes of the planar waveguide.

In the co-ordinate system shown in Figure 1(b), the dominant LP_{01} mode (the transverse electric field) of the isolated fibre is given by

$$F_0 = N_f \begin{cases} \dfrac{J_0(k_f r)}{J_0(k_f a)} & r \le a \\ \dfrac{K_0(\gamma_f r)}{K_0(\gamma_f a)} & r > a \end{cases} \quad for \tag{A2}$$

where J_0 and J_1 are the Bessel functions of the first kind, K_0 is the modified Bessel functions of the second kind and $N_f = \dfrac{\gamma_f J_0(k_f a)}{\sqrt{\pi} V_f J_1(k_f a)}$ is the normalisation constant of the fibre mode.

The parameter a denotes the fibre radius, $k_f^2 = n_f^2k^2 - \beta_{f0}^2$ and $\gamma_f^2 = \beta_{f0}^2 - n_c^2k^2$ are constants in which $k = 2\pi/\lambda$ (λ is the free-space light wavelength), β_{f0} is the propagation constant obtained from the LP_{01} mode dispersion equation[5] and n_f and n_c are the refractive indices of the fibre core and cladding respectively. $V_f = ka(n_f^2 - n_c^2)^{1/2}$ is a dimensionless waveguide parameter related to k_f and γ_f via

$$V_f^2 = a^2(k_f^2 + \gamma_f^2) \tag{A3}$$

In the same co-ordinate system (i.e. Figure 1(b)), the nth guided transverse slab mode is obtained in the form

$$S_n(x,y) =$$

$$N_s\cos(\sigma_n y)\begin{cases} V_{so}\exp[\gamma_c(x-h)]/V_{sc} & x < a+s \\ \{\cos[k_s(x-h-t)] - (\gamma_o/k_s)\sin[k_s(x-h-t)]\} & for \quad a+s \le x \le a+s+t \\ \exp[-\gamma_o(x-h-t)] & x > a+s+t \end{cases}$$

(A4)

where $n = 0, 1, 2, \cdots$, $k = 2\pi/\lambda$, $k_s^2 = n_s^2k^2 - \beta_s^2$, $\gamma_c^2 = \beta_s^2 - n_c^2k^2$, $\gamma_o^2 = \beta_s^2 - n_o^2k^2$, $V_{sc} = kt(n_s^2 - n_c^2)^{1/2}/2$, $V_{so} = kt(n_s^2 - n_o^2)^{1/2}/2$, $N_s = \left[\frac{2\gamma_c\gamma_o}{(\gamma_o + \gamma_c + \gamma_c\gamma_o t)D}\right]^{\frac{1}{2}}$ is the normalisation constant and σ_n is obtained from $\beta_{sn}^2 = \beta_s^2 - \sigma_n^2$ for n= 0,1,2…., i.e. the transverse propagation constant of the lightwaves travelling along the z-direction. The parameter t denotes the slab thickness, s the minimum distance between the surface of the fibre core and that of the polished flat (see Figure 1(b)), β_s is the propagation constant of the slab mode, n_s and n_o are the refractive indices of the slab and the overlay cladding, respectively. V_{sc} and V_{so} are dimensionless waveguide parameters related to k_s, γ_c and γ_o via

$$V_{sc}^2 = t^2(k_s^2 + \gamma_c^2)/4 \tag{A5.a}$$

$$V_{so}^2 = t^2(k_s^2+\gamma_o^2)/4 \tag{A5.b}$$

The propagation constant β_s of the slab guided mode of the m^{th} order can be obtained from the well known dispersion equation of the asymmetric planar slab waveguide

$$k_s t - \tan^{-1}(\gamma_c/k_s) - \tan^{-1}(\gamma_o/k_s) = m\pi \qquad (m = 0, 1, 2, \cdots) \tag{A6}$$

Coupled-mode equations are obtained when the field expansion (A1) is substituted into the wave equation of the total field, and then the resultant equation is multiplied successively with F_0 and S_n and integrated over the transverse (x, y) plane whilst making use of the wave equations and orthogonal relations of the fibre and slab modes. Using the scalar approximations, i.e. assuming a slowly varying envelope of the modal amplitudes and weakly coupled fibre and slab modes[10] ,both the second-order derivatives and the field overlap integrals may be neglected[11,12] and the following first-order coupled-mode equations can be obtained

$$a_0' = -j(\beta_{f00}+Q_{f00})a_0 - j\sum_n K_{f0n}\, b_n \tag{A7.a}$$

$$b_m' = -j\sum_n (\delta_{mn}\, \beta_{sn}+Q_{smn})b_n - jK_{sm0}a_0 \tag{A7.b}$$

where $a_0' = \frac{da_0}{dz}$, $b_m' = \frac{db_m}{dz}$, $m, n = 0, 1, 2, \cdots$, δ_{mn} is the Kronecker delta function, $\{Q_{f00}, Q_{smn}\}$ and $\{K_{f0n}, K_{sm0}\}$ are the self- and cross-coupling coefficients, respectively.

Conventional compound-mode equations can be obtained either from the non-orthogonal compound-mode equations by applying the scalar approximations, or straight from the above scalar coupled-mode equations by introducing a transform from the guided modes of the fibre and the slab to the compound-modes of the fibre-slab coupler:

$$A_0 = a_0 \exp(-i\beta z) \tag{A8.a}$$

$$B_n = b_n \exp(-i\beta z) \tag{A8.b}$$

The set of compound-mode equations corresponding to the set of coupled-mode equations (A7) thus becomes

$$Q_{f00}A_0 + \sum_n K_{f0n}B_n = (\beta - \beta_{f0})A_0, \tag{A9.a}$$

$$K_{sm0}A_0 + \sum_n Q_{smn}B_n = (\beta - \beta_{sm})B_m \qquad \text{for} \qquad m = 0, 1, 2, \ldots \tag{A9.b}$$

where β, the eigenvalue, and $\{A_0, B_n\ (n = 0, 1, 2, \ldots)\}$, the eigenvectors, are to be solved. The coupling coefficients in the coupled-mode and compound-mode equations, i.e. (A7.a) and (A7.b), respectively, are defined as follows

$$Q_{f00} = \frac{k^2}{2\beta_{f0}} \int_{A_\infty} [n^2(x,y) - n_f^2(x,y)] F_0 F_0 dA \tag{A10.a}$$

$$Q_{smn} = \frac{k^2}{2\beta_{sm}} \int_{A_\infty} [n^2(x,y) - n_s^2(x,y)] S_m S_n dA \tag{A10.b}$$

$$K_{f0n} = \frac{k^2}{2\beta_{f0}} \int_{A_\infty} [n^2(x,y) - n_s^2(x,y)] F_0 S_n dA \tag{A11.a}$$

$$K_{sm0} = \frac{k^2}{2\beta_{sm}} \int_{A_\infty} [n^2(x,y) - n_f^2(x,y)] S_m F_0 dA \tag{A11.b}$$

where $m, n = 0, 1, 2, \cdots$, $dA = dxdy$ and A_∞ indicates integration over the infinite cross-section, i.e. the entire transverse (x, y) plane, of the coupler system. According to the refractive index profiles as indicated in Figure 1(b) for the couplers without the grating, the coupling coefficients defined above can be categorised in two ways. $\{Q_{f00}, Q_{smn}\}$ are self coupling coefficients that represent the coupling among the fibre or slab modes due to the presence of the other, $\{K_{f0n}, K_{sm0}\}$ are cross coupling coefficients that couple the slab modes to the fibre mode and vice versa.

The above integrals can all be solved exactly except Q_{f00}, for which a large-argument asymptotic approximation of the modified Bessel function K_0 has to be used. The closed-form expressions of the coupling coefficients are given below

$$Q_{f00} = \frac{\pi^2 N_f^2 V_{sc}^2}{\sqrt{2}\beta_{f0}\gamma_f^2 t^2 \mathrm{K}_0{}^2(\gamma_f a)}[\mathrm{erf}(\sqrt{2\gamma_f(a+s+t)}) - \mathrm{erf}(\sqrt{2\gamma_f(a+s)}) + A_s \mathrm{erfc}(\sqrt{2\gamma_f(a+s+t)})]$$

(A12.a)

$$Q_{smn} = \frac{\pi N_s^2 k_s^2 V_f^2 t^2 \mathrm{e}^{-2\gamma_c(a+s)}}{8\beta_{sm} V_{sc}^2}[\frac{\mathrm{I}_1(\sqrt{4\gamma_c^2 - (\sigma_m + \sigma_n)^2}\, a)}{\sqrt{4\gamma_c^2 - (\sigma_m + \sigma_n)^2}\, a} + \frac{\mathrm{I}_1(\sqrt{4\gamma_c^2 - (\sigma_m - \sigma_n)^2}\, a)}{\sqrt{4\gamma_c^2 - (\sigma_m - \sigma_n)^2}\, a}]$$

(A12.b)

$$K_{f0n} = \frac{\pi N_f N_s V_f^2 k_s t \mathrm{e}^{-\gamma_c(a+s)}}{2\beta_{f0} a V_{sc} \mathrm{J}_0(k_f a)(k_f^2 + \gamma_c^2 - \sigma_n^2)}[\sqrt{\gamma_c^2 - \sigma_n^2}\,\mathrm{J}_0(k_f a)\mathrm{I}_1(\sqrt{\gamma_c^2 - \sigma_n^2}\, a) + k_f \mathrm{J}_1(k_f a)\mathrm{I}_0(\sqrt{\gamma_c^2 - \sigma_n^2}\, a)]$$

(A13.a)

$$K_{sn0} = \frac{\pi N_f N_s V_{sc} k_s \mathrm{e}^{-\sqrt{\gamma_f^2 + \sigma_n^2}(a+s)}}{\beta_{sn} \mathrm{K}_0(\gamma_f a) t \sqrt{\gamma_f^2 + \sigma_n^2}} \left\{ \frac{\sqrt{\gamma_f^2 + \sigma_n^2} + \gamma_c - B_s(\sqrt{\gamma_f^2 + \sigma_n^2} - \gamma_o)\mathrm{e}^{-\sqrt{\gamma_f^2 + \sigma_n^2} t}}{k_s^2 + \gamma_f^2 + \sigma_n^2} \right.$$

$$\left. + \frac{A_s B_s \mathrm{e}^{-\sqrt{\gamma_f^2 + \sigma_n^2} t}}{\gamma_o + \sqrt{\gamma_f^2 + \sigma_n^2}} \right\} \qquad \text{(A13.b)}$$

where $V_f = ka\sqrt{n_f^2 - n_c^2}$, $V_{sc} = \frac{kt}{2}\sqrt{n_s^2 - n_c^2}$, $V_{so} = \frac{kt}{2}\sqrt{n_s^2 - n_o^2}$, $A_s = \frac{n_o^2 - n_c^2}{n_s^2 - n_c^2}$, $B_s = \frac{V_{sc}}{V_{so}}$,

$B_s = \frac{V_{sc}}{V_{so}}$, erf($x$) is the error function, erfc(x) = 1 - erf(x), I_0 and I_1 are the modified Bessel functions of the first kind. In the above expressions, the new parameters A_s and B_s are introduced to quantify the geometric asymmetry of index profile of the slab waveguide. For the case involving a symmetric slab waveguide, we have $A_s = 0$ and $B_s = 1$.

FIGURE CAPTIONS

Figure 1 **(a)** *Schematic of the cross-sectional view of the grating-assisted fibre-slab coupler* **(b)** *Cross sectional view in transverse plane of the fibre-planar coupling system without grating structure.*

Figure 2. *Diagram of* $|a_0|^2$. *(a)* $n_f = 1.4817$; *(b)* $n_f = 1.475$ $t = 3\ \mu m$, $n_o = 1.40$.

(1) scalar CME without grating; (2) scalar CME incorporated with grating.

Figure 2(c) $n_f = 1.4709$, $t = 3\ \mu m$, $n_o = 1.47$. (1) scalar CME without grating; (2) scalar CME with grating.

Figure 3. *Effect of grating period.* $d = 0.05\ \mu m$, $n_o = 1.40$; *solid-lines:* $K_g = |\beta_f - \beta_{s0}|$; *dash-lines:* $K_g = |\beta_f - \beta_{s10}|$. *(1)* $n_f = 1.4756 > n_s = 1.4745$; *(2)* $n_f = 1.4709 < n_s = 1.4745$ *and (2)* $n_o = 1.46$ *and 1.47.*

Figure 4. *Effect of grating period on* $|a_0(z)|^2$. $d = 0.05\ \mu m$, $n_o = 1.40$; *solid-lines:* $K_g = |\beta_f - \beta_{s0}|$; *dash-lines:* $K_g = 2\pi/160$: (1) $n_f = 1.4756 > n_s = 1.4745$; (2) $n_f = 1.4709 < n_s = 1.4745$ and (2) $n_o = 1.46$ and *1.47*.

Figure 5 (a) and (b). *Effect of grating period on* $|a_0(z)|^2$. $d = 0.05\ \mu m$; (a) $n_o = 1.46$; (b) $n_o = 1.47$. Solid-lines: $K_g = |\beta_f - \beta_{s0}|$; Dash-lines: $K_g = 2\pi/160$. (1) $n_f = 1.4756 > n_s = 1.4745$; (2) $n_f = 1.4709 < n_s = 1.4745$.

Figure 6 Effects of grating depth. $K_g = |\beta_f - \beta_{s0}|$; solid lines: d =0.05 μm; dash-lines: d =0.025 μm. (1) $n_f = 1.4756 > n_s = 1.4745$; (2) $n_f = 1.4709 < n_s = 1.4745$.

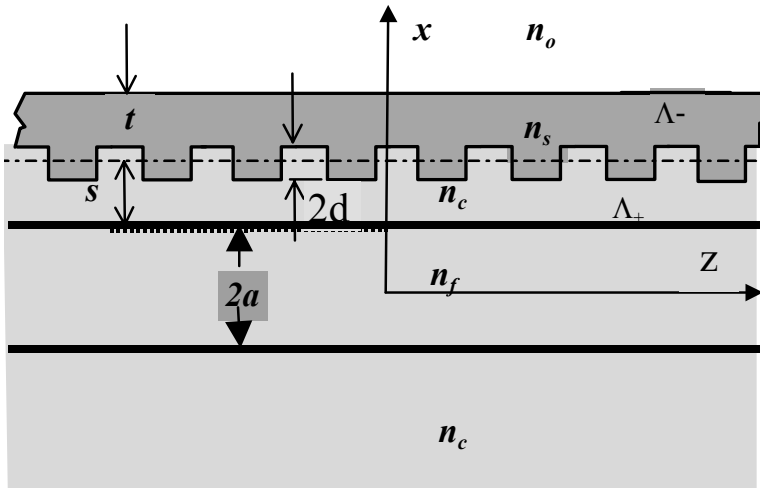

(a)

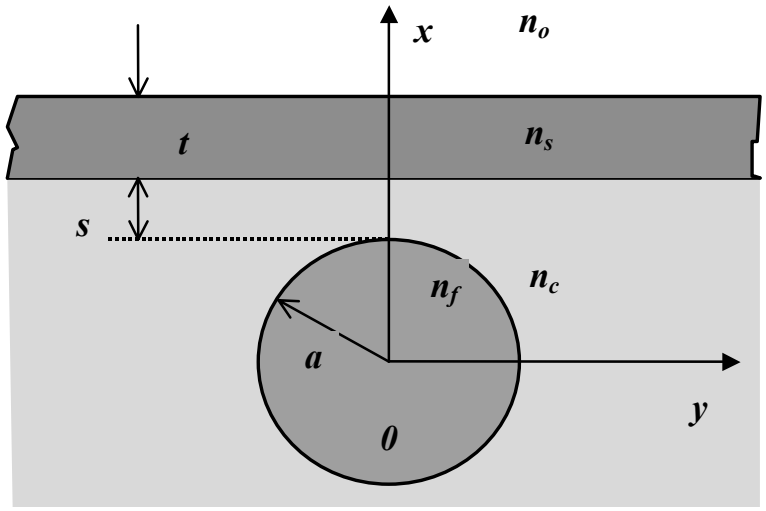

(b)

Figure 1. ***(a)****Schematic of the cross-sectional view along the propagation direction of the grating-assisted fibre-slab coupler (b) Cross sectional view in transverse plane of the fibre-planar coupling system without grating structure.*

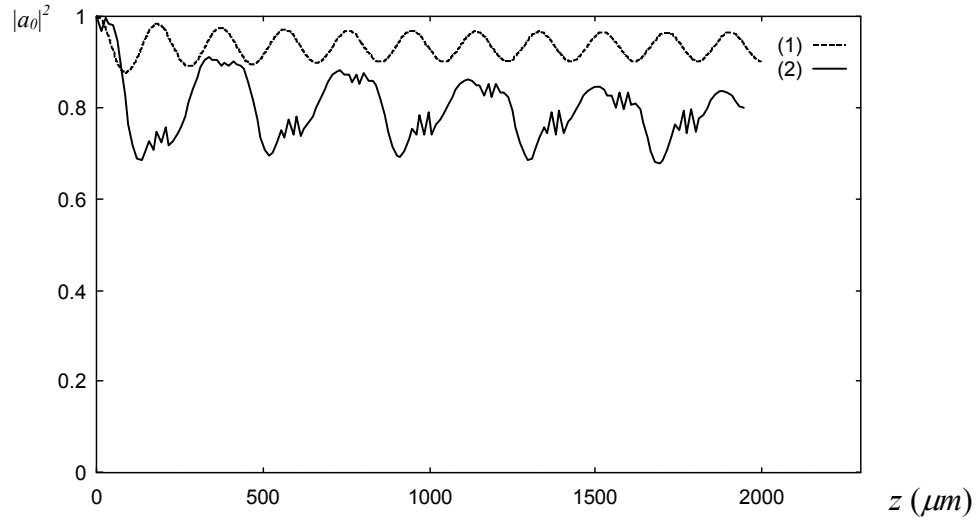

Figure 2(a)

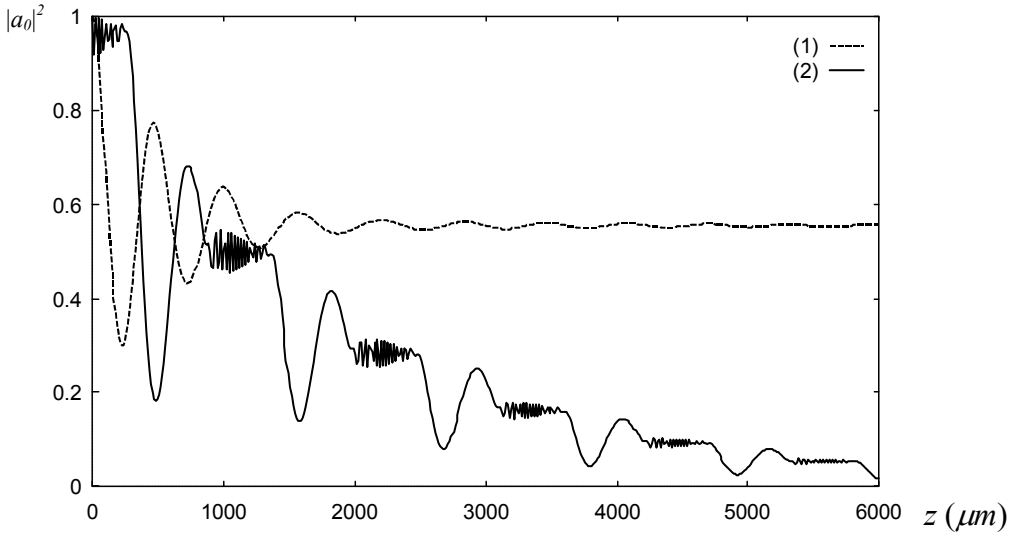

Figure 2(b)

Figure 2. *Diagram of* $|a_0|^2$. *(a)* $n_f = 1.4817$; *(b)* $n_f = 1.475$ $t = 3\ \mu m$, $n_o = 1.40$.

(1) scalar CME without grating; (2) scalar CME with grating.

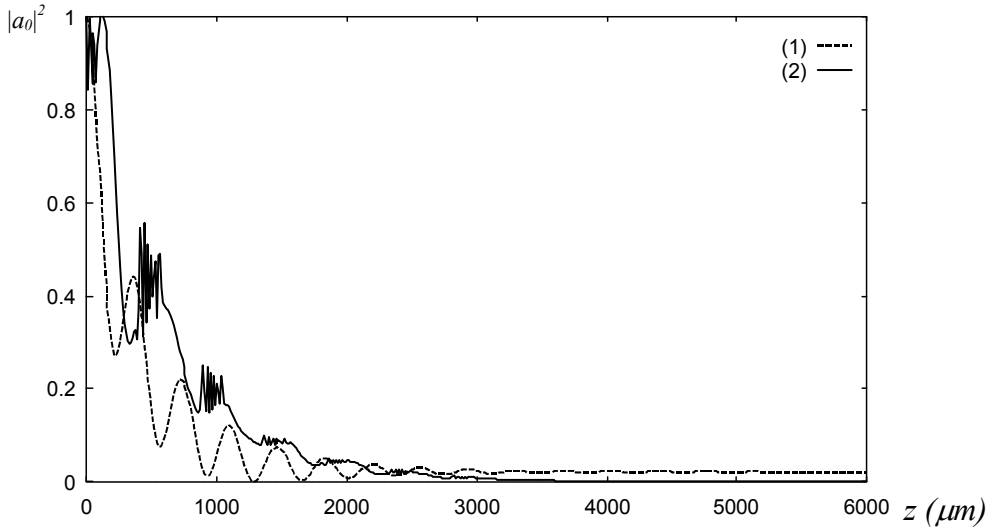

Figure 2(c) *n_f = 1.4709, t = 3 μm, n_o = 1.47.* (1) scalar CME without grating; (2) scalar CME with grating.

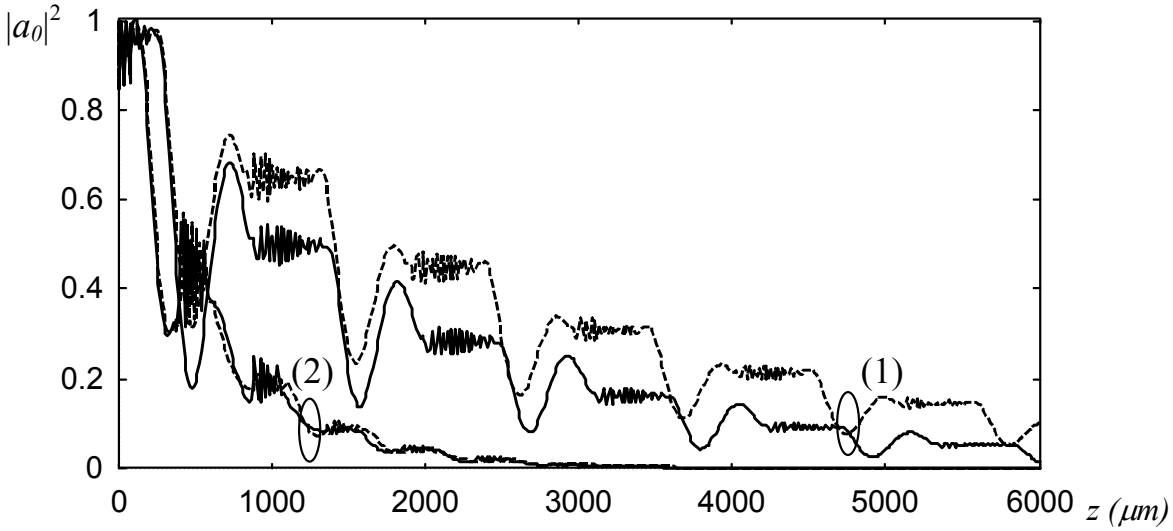

Figure 3. *Effect of grating period. d = 0.05 μm, n_o= 1.40; solid-lines: $K_g = |\beta_f - \beta_{s0}|$; dash-lines: $K_g = |\beta_f - \beta_{s10}|$. (1) n_f = 1.4756 > n_s = 1.4745; (2) n_f = 1.4709 < n_s = 1.4745 and (2) n_o= 1.46 and 1.47.*

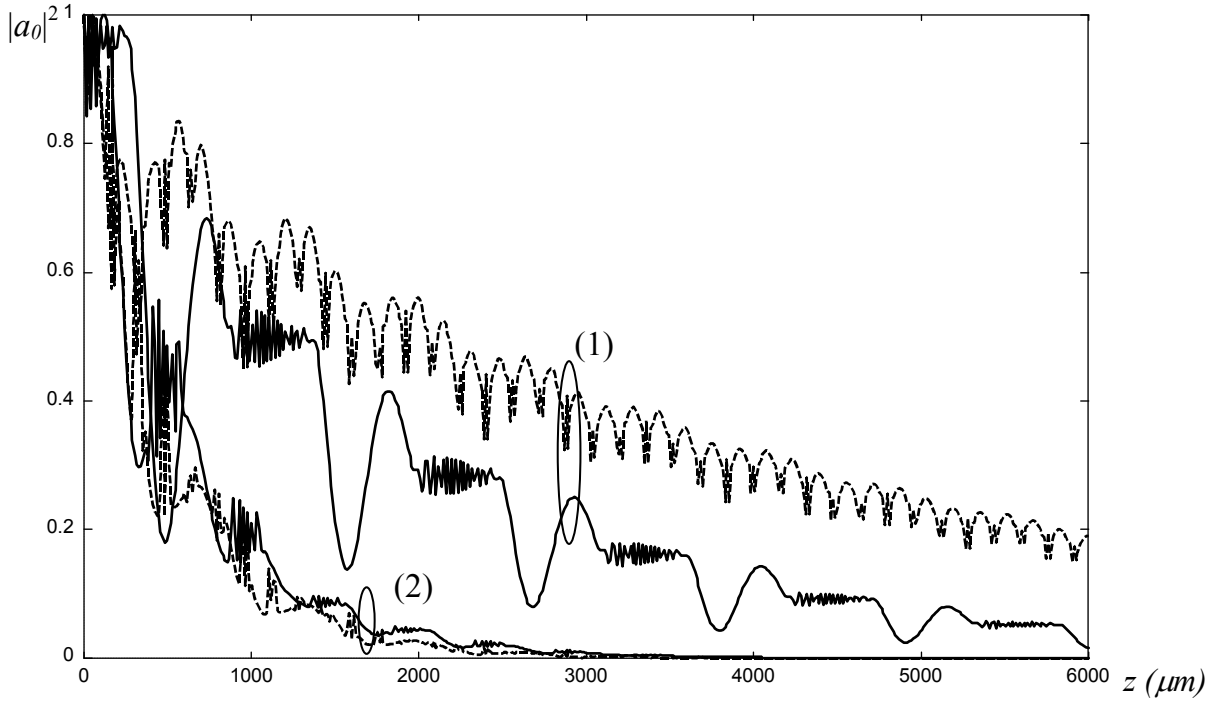

Figure 4. Effect of grating period on $|a_0(z)|^2$. d = 0.05 μm, n_o= 1.40; solid-lines: $K_g = |\beta_f - \beta_{s0}|$; dash-lines: $K_g = 2\pi/160$: (1) $n_f = 1.4756 > n_s = 1.4745$; (2) $n_f = 1.4709 < n_s = 1.4745$ and (2) n_o= 1.46 and 1.47.

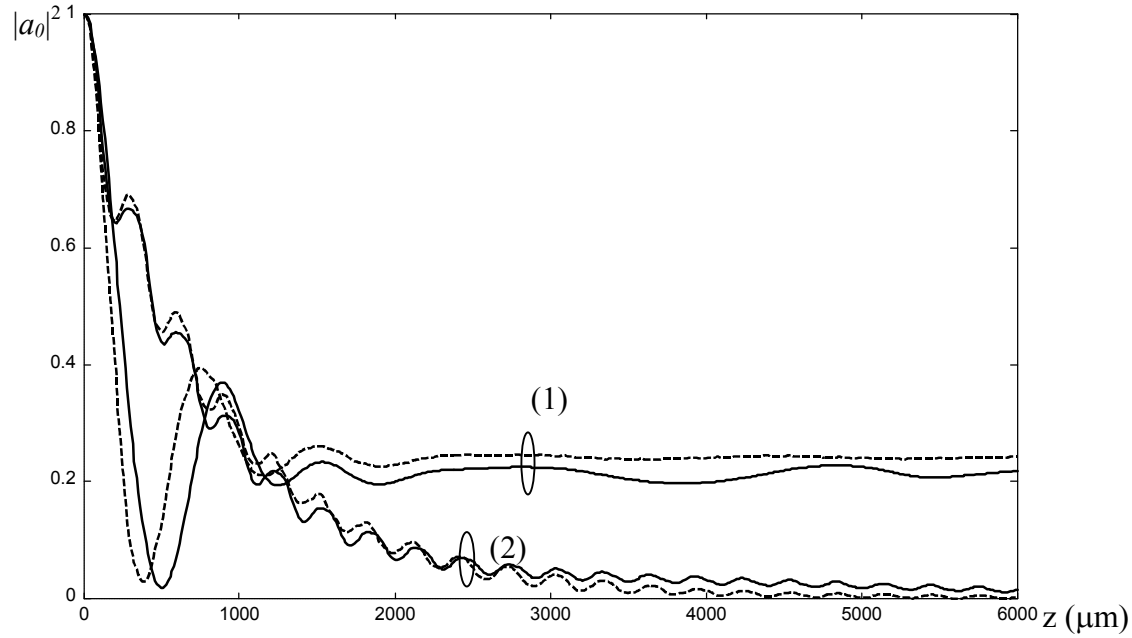

Figure 5(a)

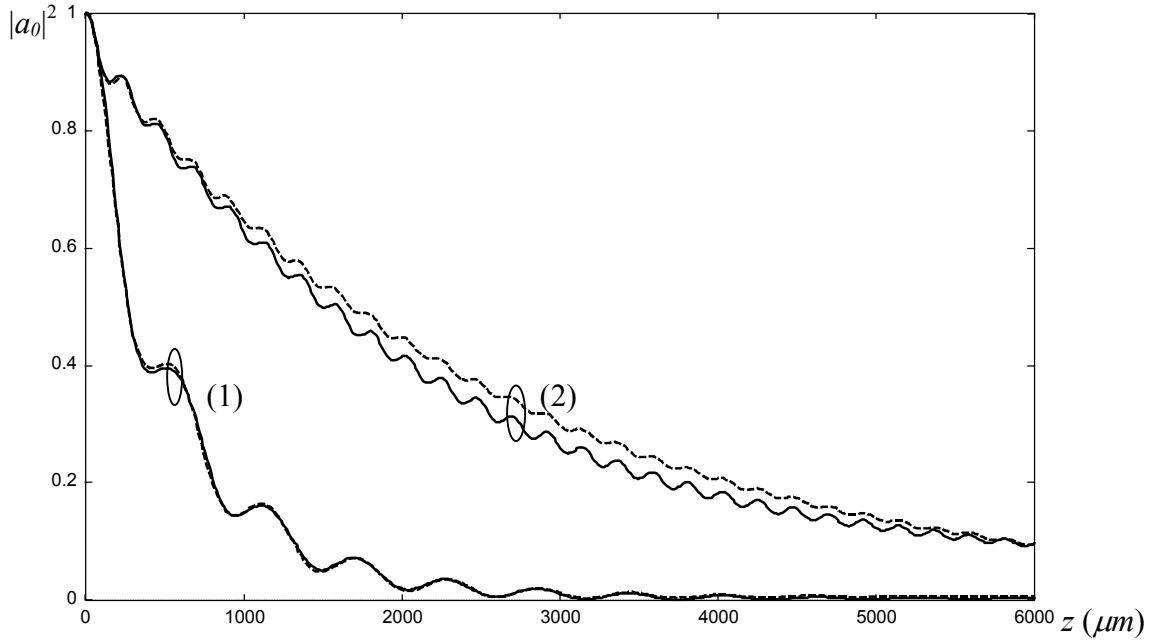

Figure 5(b)

Figure 5 (a) and (b)*. Effect of grating period on $|a_0(z)|^2$. d =0.05 μm;* (a) n_o= 1.46; (b) n_o= 1.47. Solid-lines: $K_g = |\beta_f - \beta_{s0}|$; Dash-lines: $K_g = 2\pi/160$. (1) $n_f = 1.4756 > n_s = 1.4745$; (2) $n_f = 1.4709 < n_s = 1.4745$.

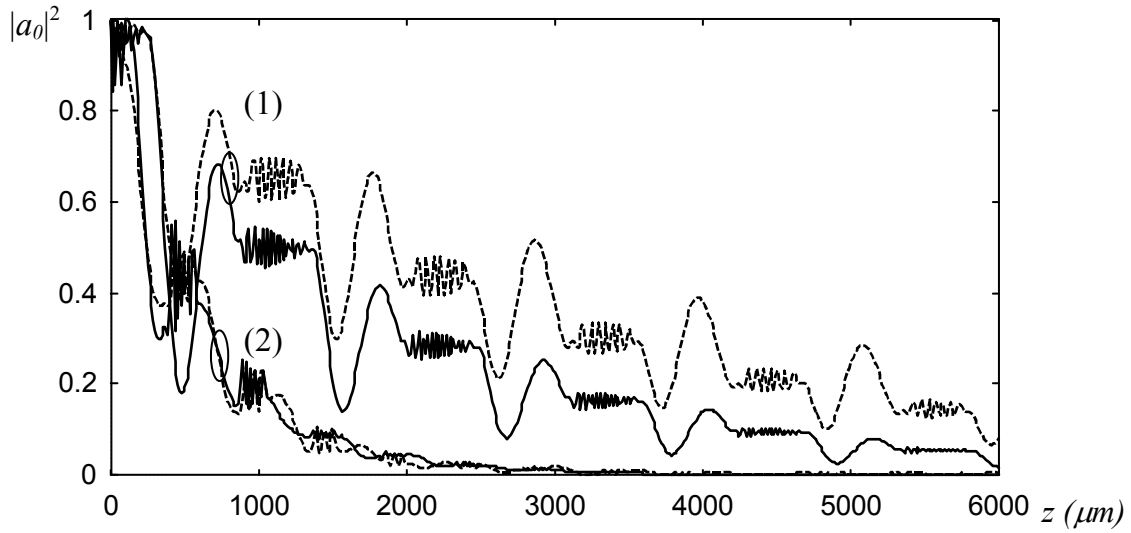

Figure 6 Effect of grating depth. $K_g = |\beta_f - \beta_{s0}|$; solid lines: d =0.05 μm; dash-lines: d =0.025 μm. (1) $n_f = 1.4756 > n_s = 1.4745$; (2) $n_f = 1.4709 < n_s = 1.4745$.